



## Coupling of highly exothermic and endothermic reactions in a metallic monolith catalyst reactor: A preliminary experimental study

Fengxiang Yin, Shengfu Ji\*, Hong Mei, Zhongliang Zhou, Chengyue Li\*

State Key Laboratory of Chemical Resource Engineering, Beijing University of Chemical Technology, 15 Beisanhuan Dong Road, P.O. Box 35, Beijing 100029, China

### ARTICLE INFO

#### Article history:

Received 9 November 2008

Received in revised form 19 March 2009

Accepted 19 March 2009

#### Keywords:

Catalysis

Chemical reactors

Catalyst support

Combustion

Coupling of exothermic/endothermic reactions

Reforming of methane with CO<sub>2</sub>

### ABSTRACT

An LaFe<sub>0.5</sub>Mg<sub>0.5</sub>O<sub>3</sub>/Al<sub>2</sub>O<sub>3</sub>/FeCrAl metallic monolith catalyst for the exothermic catalytic combustion of methane and an Ni/SBA-15/Al<sub>2</sub>O<sub>3</sub>/FeCrAl metallic monolith catalyst for the endothermic reforming of methane with CO<sub>2</sub> have been prepared. A laboratory-scale tubular jacket reactor with the Ni/SBA-15/Al<sub>2</sub>O<sub>3</sub>/FeCrAl catalyst packed into its outer jacket and the LaFe<sub>0.5</sub>Mg<sub>0.5</sub>O<sub>3</sub>/Al<sub>2</sub>O<sub>3</sub>/FeCrAl catalyst packed into its inner tube was devised and constructed. The reactor allows a coupling of the exothermic and endothermic reactions by virtue of their thermal matching. An experimental study in which the temperature difference between the chamber of the external electric furnace and the metallic monolith catalyst bed in the jacket was kept very small, by adjusting the power supply to the furnace, confirmed that the heat absorbed in the reforming reaction does indeed partly come from that evolved in the catalytic combustion of methane, and that the direct thermal coupling of the two reactions in the reactor can be realized in practice. When the temperature of the electric furnace chamber was 1088 K, and the gas hourly space velocities (GHSVs) of the reactant mixtures passed through the inner tube and the jacket were 382 h<sup>-1</sup> and 40 h<sup>-1</sup>, respectively, the conversions of methane and CO<sub>2</sub> in the reforming reaction were 93.6% and 91.7%, respectively, and the heat efficiency reached 81.9%. Stability tests showed that neither catalyst underwent deactivation during 150 h on stream.

© 2009 Elsevier B.V. All rights reserved.

### 1. Introduction

Process intensification can reduce equipment size, increase the utilization of energy and reduce environmental impact, and therefore has been widely studied. A novel reactor concept, which facilitates direct coupling of highly exothermic and endothermic reactions, is one example of process intensification which has attracted great attention [1–3]. Since the exothermic and endothermic reactions take place simultaneously in the same fixed-bed reactor, the equipment size can be markedly reduced and the utilization efficiency of energy and resources can be significantly improved. A variety of coupling schemes have been reported in the literature [3–6]. The simplest system involves an exothermic reaction and an endothermic reaction being run in parallel over a mixed catalyst in a single bed [7–11], but a catalyst that promotes both the endothermic and exothermic reactions in the same temperature range is obviously required in such a system, which limits its application. A bi-directional fixed-bed reactor concept has also been developed [12–14]. During the exothermic semi-cycle the fixed bed is heated and the stored heat is consumed in the next semi-cycle when the endothermic reac-

tion takes place. In this system, however, the dynamic behavior of the reactor is complicated and inefficient heat integration can cause hot spots. In order to overcome these problems, a spatially segregated system that allows indirect heat exchange through a thermally conductive substrate has been proposed as an alternative. The exothermic and endothermic reactions take place in different parts of the system and the reactants can flow in co- or counter-current manner in the reaction zones. Both tubular heat-exchanging reactors [15–17] and catalytic plate reactors (CPR) have been proposed [18–22]. In the latter case, the catalysts for exothermic and endothermic reactions are loaded on opposite surfaces of a plate. The influences of varying wall thickness, thermal conductivity, catalyst loading, reaction temperature, and reactant composition and flow rates on the reactor behavior have been studied in detail by means of simulations. In most of the coupled systems which have been studied to date, the highly exothermic reactions involve combustion of hydrocarbons, with the endothermic reactions being reforming, cracking or dehydrogenation of hydrocarbons. Owing to thermodynamic and kinetic limitations, these strongly endothermic reactions have to be carried out at high temperature, which means that the reactors used in these systems must possess excellent heat transfer properties so that the heat absorbed in the endothermic reactions can be supplied efficiently. In the cases of conventional reactors placed in an oven, the reactions can be facilitated by direct heating. However, the equip-

\* Corresponding authors. Tel.: +86 10 64412054; fax: +86 10 64419619.

E-mail addresses: [jjsf@mail.buct.edu.cn](mailto:jjsf@mail.buct.edu.cn) (S. Ji), [licy@mail.buct.edu.cn](mailto:licy@mail.buct.edu.cn) (C. Li).

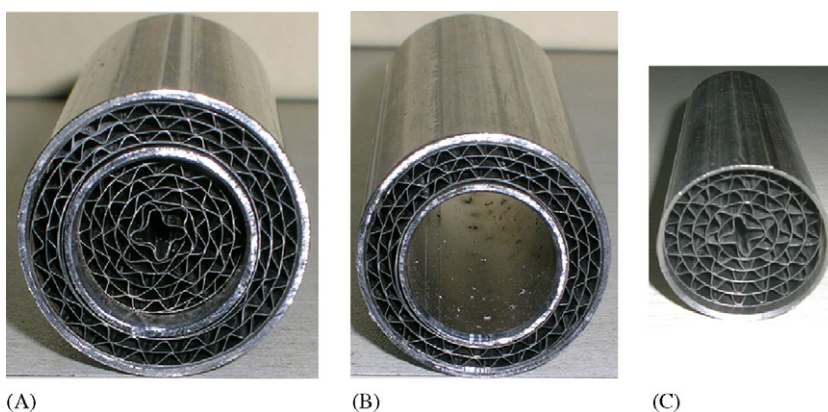


**Fig. 1.** The assembled monolith support reactor and its annular and inner components. A: The assembled monolith support reactor; B: Annular component; C: Inner component.

ment is complicated and the utilization efficiency of energy is very low.

In recent years, monolith catalysts and reactors which use metallic monoliths as the support have attracted considerable attention [23,24]. These catalysts and reactors have much better heat and mass transfer performance and much lower pressure drop compared with a conventional pellet-packed bed. They can also be constructed with a variety of flow channels and specific surface area according to the requirements of a given reaction system. Therefore, metallic monolith catalysts have considerable potential for application in the coupling of highly exothermic and strongly endothermic reactions. In our previous work, a series of metallic monolith catalysts with a honeycomb structure were prepared and characterized, and their catalytic performances were evaluated [25–27]. Modeling and simulation studies of the mass and heat transfer performances of the metallic monolith catalyst as well as the performance of a tubular heat-exchanging reactor in coupling of the catalytic combustion of methane with methane steam reforming confirmed the feasibility of the coupling [28,29]. In this work, preliminary data on the performance of a tubular jacket reactor packed with metallic monolith catalysts devised for coupling the catalytic combustion of methane – the concentration of which is under the explosive limit – with its  $\text{CO}_2$  reforming are reported.

## 2. Experimental

### 2.1. Catalyst preparation

The assembled metallic monolith catalyst tubular jacket reactor is shown in Fig. 1A and the annular and inner components of the reactor are illustrated in Fig. 1B and C, respectively. Metallic monolith catalysts were prepared by coating washcoat layers and depositing the active phases on the channel walls of monolith supports. The preparation of various metallic monolith catalysts used in the catalytic combustion of methane has been described in detail elsewhere [25–27].  $\text{LaFe}_{0.5}\text{Mg}_{0.5}\text{O}_3$  has been shown to be an active and stable catalyst for the catalytic combustion of methane [26] and was selected as active phase of the catalyst in the inner tube of the reactor. The loading of  $\text{LaFe}_{0.5}\text{Mg}_{0.5}\text{O}_3/\text{Al}_2\text{O}_3$  was 30 wt.% of the whole catalyst. The loading of  $\text{LaFe}_{0.5}\text{Mg}_{0.5}\text{O}_3$  was 8 wt.% based on the weight of  $\text{LaFe}_{0.5}\text{Mg}_{0.5}\text{O}_3/\text{Al}_2\text{O}_3$ . Thus, the loading of  $\text{LaFe}_{0.5}\text{Mg}_{0.5}\text{O}_3$  was 2.4 wt.% and the loading of  $\text{Al}_2\text{O}_3$  was 27.6 wt.% based on the weight of whole catalyst.

As shown in previous work [30], an Ni/SBA-15 catalyst prepared by assembling the active Ni phase in the channels of SBA-15 exhibited excellent catalytic performance for the reforming of methane with  $\text{CO}_2$ , because sintering of the active phase is prevented by

virtue of the limitations imposed by the channel walls. In this work, the annular metallic monolith catalyst used for reforming of methane with  $\text{CO}_2$ , Ni/SBA-15/ $\text{Al}_2\text{O}_3$ /FeCrAl, was prepared by supporting the Ni/SBA-15 catalyst on the  $\text{Al}_2\text{O}_3$ /FeCrAl monolith support. The  $\text{Al}_2\text{O}_3$ /FeCrAl monolith support was coated with an Ni/SBA-15 slurry, then dried at room temperature in air and finally calcined at  $500^\circ\text{C}$  for 4 h. Higher loadings were obtained by repeating the coating procedure. The loading of Ni/SBA-15/ $\text{Al}_2\text{O}_3$  was 30 wt.% of the whole catalyst, of which the loading of Ni/SBA-15 was 20 wt.% and the loading of  $\text{Al}_2\text{O}_3$  was 10 wt.%. The loading of Ni was 25 wt.% based on the weight of Ni/SBA-15. Thus based on the weight of whole catalyst, the loading of Ni was 5 wt.% and the loading of SBA-15 was 15 wt.%.

The inner tube and jacket of the tubular jacket reactor into which the monolith catalysts were packed had interior diameter of 20 mm and length of 100 mm, and external diameter of 34 mm and length of 100 mm, respectively.

### 2.2. Experimental set-up and procedure

A flow chart of the experimental set-up for coupling of the exothermic and endothermic reactions is shown in Fig. 2. The reactants flow downwards in a co-current manner. Thermocouples T1 and T2 were placed in the center of the inner and the annular monolith catalyst beds, respectively. In a preliminary experiment, the thermocouples T1 and T2 were moved axially and it was found that the axial temperature profiles of the two catalyst beds were approximately uniform, with the axial temperature variation being less than 1 K; this is a result both of the excellent heat transfer properties of the metallic monolith catalysts and the catalyst beds being significantly shorter than the chamber length of the electric furnace. In view of the very short catalyst beds, it is not necessary to balance the heat transfer axially and radially for the coupled exothermic/endothermic reactions. Therefore the temperatures measured by T1, T2 and T3, respectively, can be assumed to accurately represent those of the inner catalyst bed, the annular catalyst bed and the chamber of the electric furnace at the same horizontal position. Prior to the experiment, the furnace chamber temperature was raised to the required value and then the  $\text{CH}_4/\text{air}$  mixture, in which the concentration of methane was 3.5 vol.% (under the explosive limit), was introduced with a flow rate ranging from  $191\text{ h}^{-1}$  to  $955\text{ h}^{-1}$  into the inner catalyst bed. The reaction was stabilized for a period of time after the conversion of methane reached close to 100%. The chamber temperature of the electric furnace was then raised to  $800^\circ\text{C}$  and  $\text{H}_2$  with a flow rate of  $40\text{ h}^{-1}$  was introduced into the annular catalyst bed in order to bring about reduction of the nickel catalyst. After reduction for 5 h,  $\text{H}_2$  was replaced by  $\text{N}_2$  in

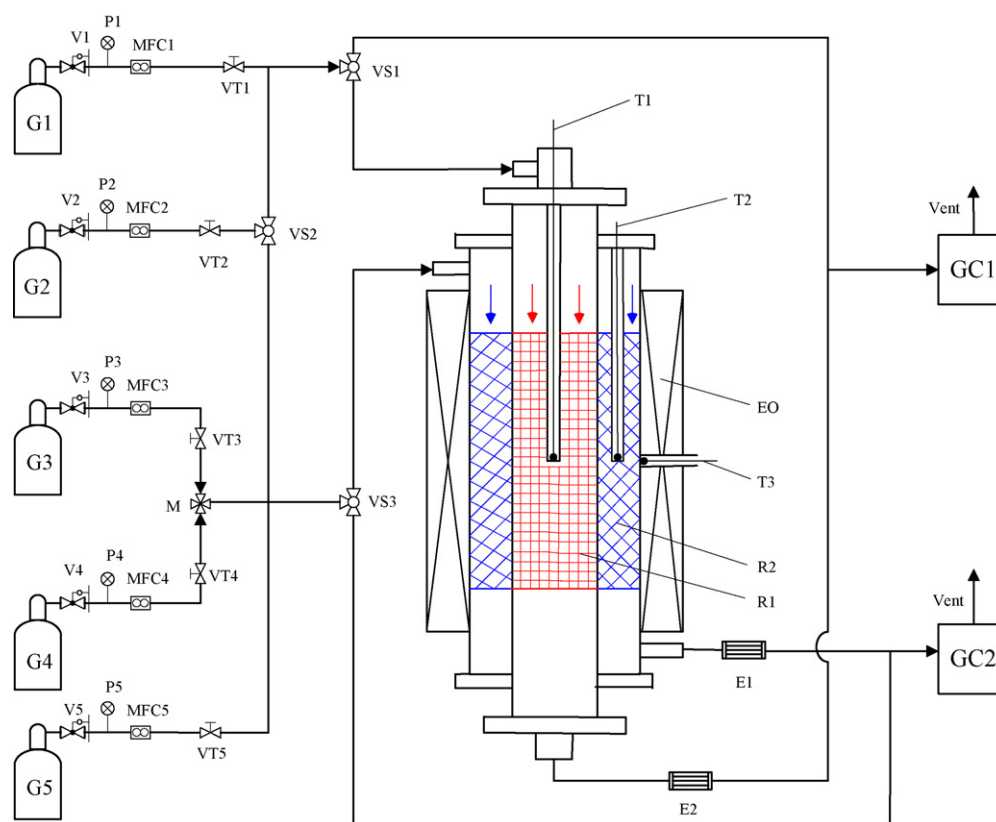
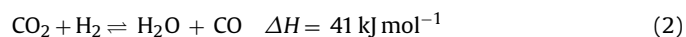
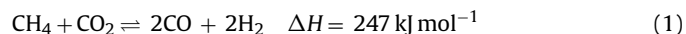


**Fig. 2.** Flow chart of the experimental set-up for coupling the two reactions. G1: 3.5 vol.% CH<sub>4</sub>/air; G2: N<sub>2</sub>; G3: CH<sub>4</sub>; G4: CO<sub>2</sub>; G5: H<sub>2</sub>; V1–V5: pressure relief valves; P1–P5: pressure indicators; MFC1–MFC5: mass flow controllers; VT1–VT5: shut down valves; M: mixer; VS1–VS3: two-position three-way valves; T1–T3: thermocouples; EO: electric oven; R1: inner metallic monolith catalyst; R2: annular metallic monolith catalyst; E1–E2: condensers; GC1–GC2: gas chromatographs.

order to sweep the pipelines. The furnace chamber temperature was then adjusted to the required value for reaction, the N<sub>2</sub> was shut off, and the reactant mixture (CH<sub>4</sub>/CO<sub>2</sub>, molar ratio 1:1) with a flow rate ranging from 20 h<sup>-1</sup> to 152 h<sup>-1</sup> was introduced into the annular catalyst bed. The temperature of the furnace chamber was maintained approximately equal to that of the annular catalyst bed by adjusting the input voltage of the furnace as necessary. All experiments were carried out at atmospheric pressure.

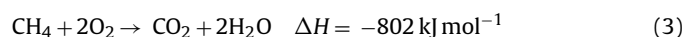
The compositions of the reactant and product of the two reactions were measured on-line by two gas chromatographs equipped with thermal conductivity detectors (Beijing East & West Electronics Institute, GC-4000A). The product was condensed in a cold trap before reaching the detector.

The main reactions occurring over the Ni/SBA-15/Al<sub>2</sub>O<sub>3</sub>/FeCrAl metallic monolith catalyst are as follows:



The conversions of methane and CO<sub>2</sub> as well as the molar ratio of H<sub>2</sub> to CO were calculated from Eqs. (S1), (S2) and (S3) in the Supplementary Material.

The catalytic combustion of methane is shown in Eq. (3).



The degree of carbon balance can be taken as an indicator of the veracity of the experimental results and was observed to be higher than 95% in each case.

### 3. Results and discussion

#### 3.1. Performance of the metallic monolith catalysts

Prior to the coupling experiments, the catalytic combustion reaction of methane over the inner catalyst bed and methane reforming with CO<sub>2</sub> over the annular catalyst bed were carried out separately in order to evaluate the performance of the two catalysts. The results are shown in Figs. S1–S4 in the Supplementary Material. For a flow rate of 382 h<sup>-1</sup>, the conversion of methane in its catalytic combustion reached 100% at a furnace chamber temperature of 986 K, and at a fixed furnace chamber temperature of 1088 K the complete conversion of methane was essentially observed for flow rates ranging from 191 h<sup>-1</sup> to 955 h<sup>-1</sup>. For the reforming reaction, at a furnace chamber temperature of 1088 K or above the conversions of methane and CO<sub>2</sub> were higher than 91% and the molar ratio of H<sub>2</sub> to CO in the product gas was close to unity. These results confirm that the catalysts selected have satisfactory activities for the catalytic combustion of methane and methane reforming with CO<sub>2</sub> under the experimental conditions.

#### 3.2. Influence of varying the reaction conditions on the coupling process

##### 3.2.1. Influence of varying the flow rate of the reactant mixture through the outer jacket

A fixed furnace chamber temperature of 1088 K and a fixed flow rate of reactant mixture through the inner catalyst bed of 764 h<sup>-1</sup> were chosen in order to investigate the effects of varying the flow rate of reactant mixture through the jacket (annular catalyst bed) on the performance of the coupled system. Catalytic combustion of methane over the inner catalyst bed was found to be complete in

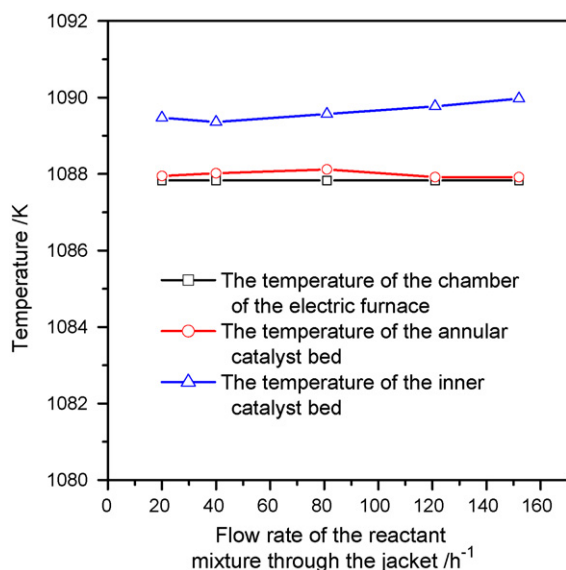


**Fig. 3.** Influence of the flow rate of the reactant mixture through the jacket on the temperature of the inner and annular catalyst beds. (The temperature of the chamber of the electric furnace was 1088 K and the flow rate of the reactant mixture through the inner tube was 764 h<sup>-1</sup>.)

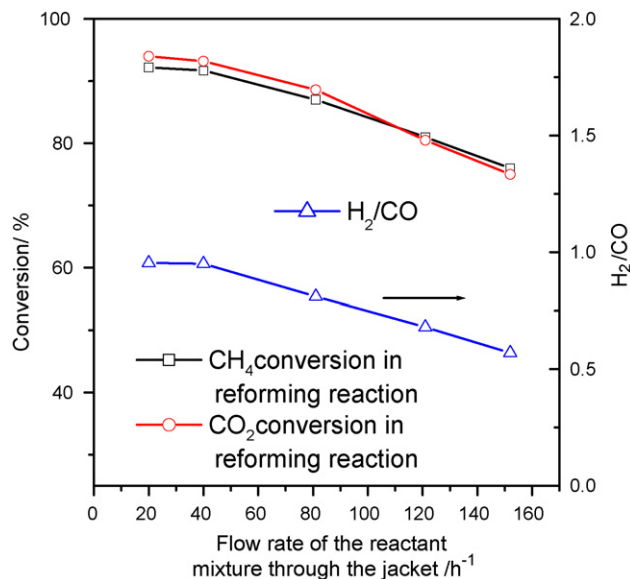
all the experiments. Fig. 3 shows that, at a fixed furnace chamber temperature, the temperatures of the inner and annular catalyst beds were essentially independent of the flow rate of the reactant mixture through the jacket in the range from 20 h<sup>-1</sup> to 152 h<sup>-1</sup>. In addition, the temperature of the annular catalyst bed was very close to that of the furnace chamber because the variation in amount of heat absorbed by the endothermic reaction with flow rate of the reactant mixture through the jacket was relatively small in comparison with the thermal capacity of the electric furnace. However the temperature of the inner catalyst bed was significantly higher than those of the annular catalyst bed and the furnace chamber. This indicates that the heat absorbed by the reforming reaction was indeed partly provided by the catalytic combustion of methane via radial heat transfer between the inner and the annular catalyst beds. It should be noted that the temperature of the furnace body will be slightly higher than that of furnace chamber (and the annular catalyst bed) so that there will also be radiative heat transfer from the furnace body to the reactor.

Fig. 4 shows the effects on the reforming reaction of varying the flow rate of the reactant mixture through the jacket. The conversions of methane and CO<sub>2</sub> as well as the molar ratio of H<sub>2</sub> to CO in the product gas all decreased with increasing flow rate. The main reason for the reduction in conversion of methane and CO<sub>2</sub> is that the contact time decreases with increasing flow rate. Furthermore, the reverse water-gas shift reaction can also occur over the annular catalyst bed, which consumes H<sub>2</sub> produced in the reforming reaction and produces CO and H<sub>2</sub>O, resulting in the observed decrease in the molar ratio of H<sub>2</sub> to CO.

### 3.2.2. Influence of varying the flow rate of the reactant mixture through the inner catalyst bed

The flow rate of the reactant mixture through the inner catalyst bed was varied while maintaining the flow rate of the reactant mixture through the jacket at 40 h<sup>-1</sup> and the furnace chamber temperature at 1088 K. In each case, catalytic combustion of methane was found to be complete.

Fig. 5 shows that the temperatures of the inner and the annular catalyst beds were essentially independent of the flow rate of the reactant mixture through the inner catalyst bed. This is because the heat capacity of the electric furnace is very large compared with the



**Fig. 4.** Influence of the flow rate of the reactant mixture through the jacket on the reforming reaction. (The temperature of the chamber of the electric furnace was 1088 K and the flow rate of the reactant mixture through the inner tube was 764 h<sup>-1</sup>.)

changes in the amount of reaction heat evolved which result from varying the flow rate. The temperature of the annular catalyst bed was very close to that of the furnace chamber, but the temperature of the inner catalyst bed was slightly higher. As mentioned above, this suggests that the heat absorbed by the reforming reaction is partly provided by the heat evolved in the catalytic combustion of methane via radial heat transfer through the inner and the annular catalyst beds, although the heat transferred from the furnace body to the reactor, which cannot be measured accurately, will also make a contribution.

The effects of varying the flow rate of reactant mixture through the inner tube on the reforming reaction are shown in Fig. 6. It can be seen that there was no significant change in either the conversions of methane and CO<sub>2</sub> or in the molar ratio of H<sub>2</sub> to CO, which is as expected on the basis of the above discussion.

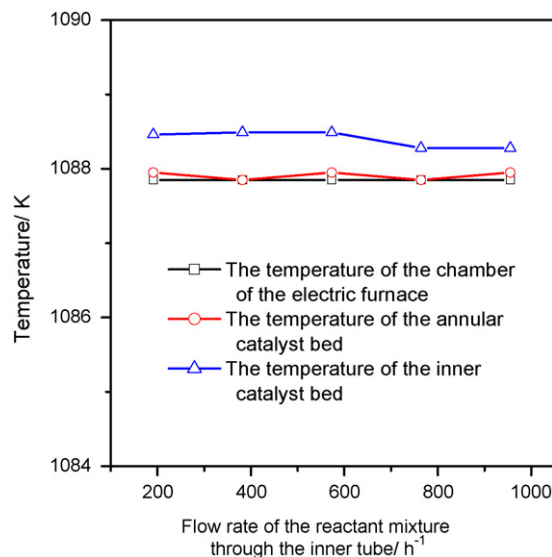


**Fig. 5.** Influence of the flow rate of the reactant mixture through the inner tube on the temperature of the inner and annular catalyst beds. (The temperature of the chamber of the electric furnace was 1088 K and the flow rate of the reactant mixture through the jacket was 40 h<sup>-1</sup>.)

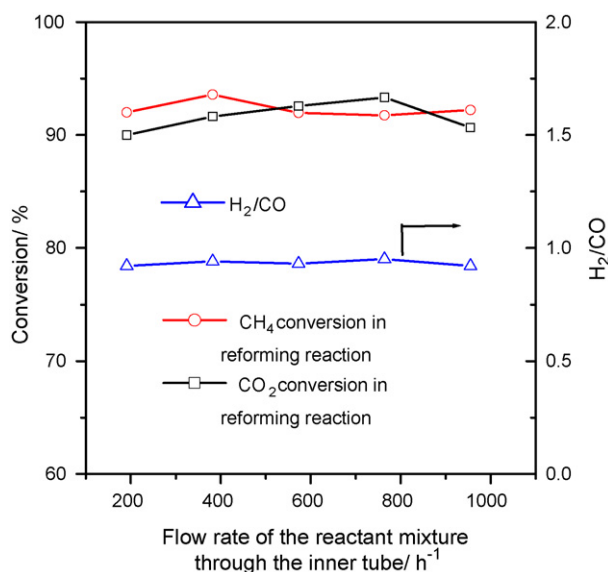


**Fig. 6.** Influence of the flow rate of the reactant mixture through the inner tube on the reforming reaction. (The temperature of the chamber of the electric furnace was 1088 K and the flow rate of the reactant mixture through the jacket was 40 h<sup>-1</sup>.)

### 3.2.3. Influence of varying the reaction temperature

As noted above, during the coupling experiments the temperature of the furnace chamber was very close to that of the annular catalyst bed while the temperature of the inner catalyst bed was slightly higher than those of the furnace chamber and the annular catalyst bed. Therefore the furnace chamber temperature is good representation of the temperature in the reactor. Fig. 7 shows the effects of increasing the temperature of the furnace chamber on the temperatures of the catalyst beds for fixed flow rates of the reactant mixtures through the annular and the inner catalyst beds. When the temperature of the furnace chamber was increased from 986 K to 1139 K, there were corresponding increases in the temperatures of the inner and the annular catalyst beds. The temperature

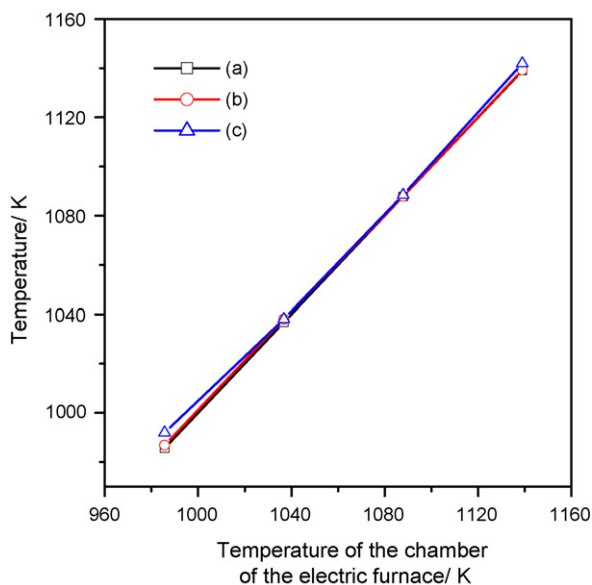


**Fig. 7.** Influence of the temperature of the chamber of the electric furnace on the temperatures of the inner and annular catalyst beds. (a) The temperature of the chamber of the electric furnace; (b) The temperature of the annular catalyst bed; (c) The temperature of the inner catalyst bed. (The flow rates of the reactant mixtures through the jacket and inner tube were 40 h<sup>-1</sup> and 382 h<sup>-1</sup>, respectively.)

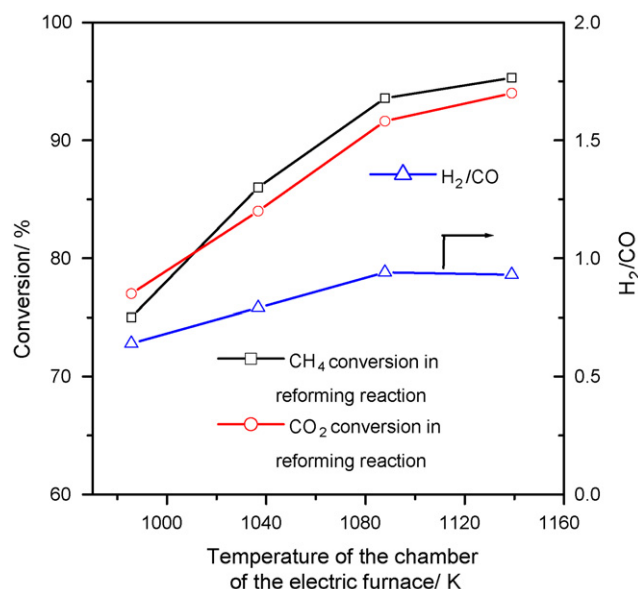


**Fig. 8.** Influence of the temperature of the chamber of the electric furnace on the reforming reaction. (The flow rates of the reactant mixtures through the jacket and inner tube were 40 h<sup>-1</sup> and 382 h<sup>-1</sup>, respectively.)

of the inner catalyst bed was always slightly higher than those of the annular catalyst bed and the furnace chamber. The observed temperature difference between the annular catalyst bed and the furnace chamber was very small, particularly at higher temperatures, because the heat of reaction is very small in comparison with the thermal capacity of the electric furnace.

Fig. 8 shows the effect of increasing the temperature of the furnace chamber on the reforming reaction, with fixed flow rates of reactants through the jacket and inner tube. In all cases, the conversion of methane was close to 100%. The conversions of methane and CO<sub>2</sub> in the reforming reaction as well as the molar ratio of H<sub>2</sub> to CO all increased significantly when the temperature of the furnace chamber was raised from 986 K to 1088 K, and then increased more slowly when the temperature was raised further, as the system approached the thermodynamic limit. The same behavior is seen in a conventional reactor for a reversible endothermic reaction such as the reforming reaction. When the temperature of the furnace chamber was 1088 K, the conversions of methane and CO<sub>2</sub> in the reforming reaction reached 93.6% and 91.7%, respectively.

### 3.2.4. Heat efficiency and equilibrium temperature difference

In order to evaluate the efficiency of utilization of the reaction heat evolved in the exothermic reaction, we define a heat efficiency of the reactor,  $\eta$ . Since the temperature of the furnace chamber was maintained approximately equal to that of the annular catalyst bed during the coupling experiments, the heat exchange between the reactor and the furnace can be considered to be negligible and the heat efficiency  $\eta$  can be calculated according to the following equation:

$$\eta = \frac{\Delta Q_1}{\Delta Q_2} \times 100\% \quad (4)$$

where  $\Delta Q_1$  is the heat absorbed by the annular catalyst bed and  $\Delta Q_2$  is the heat evolved in the inner catalyst bed. Based on the general principles governing the thermal balance of chemical reactions,  $\Delta Q_1$  and  $\Delta Q_2$  can be calculated.

Because the reforming of methane with CO<sub>2</sub> is a reversible reaction, the temperature difference from equilibrium should be considered as an indication of the degree of departure from

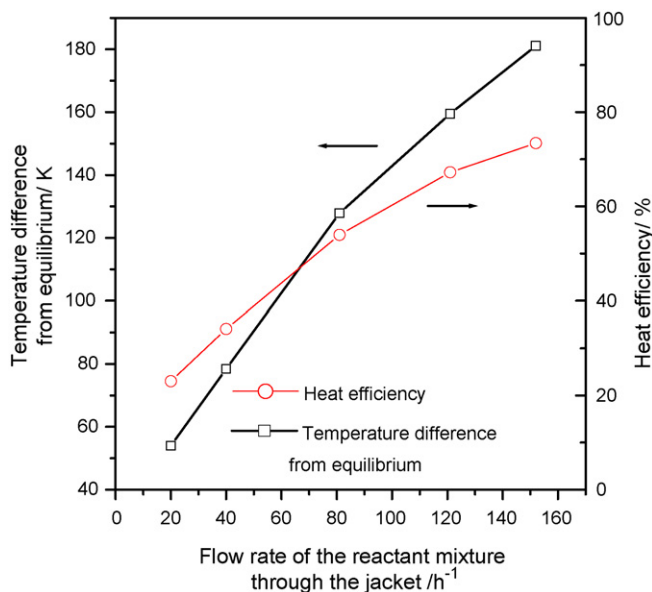


**Fig. 9.** Influence of the flow rate of the reactant mixture through the jacket on the heat efficiency and the temperature difference from equilibrium. (The temperature of the chamber of the electric furnace was 1088 K and the flow rate of the reactant mixture through the inner tube was 764 h<sup>-1</sup>.)

chemical equilibrium of the reaction system. Starting from the Gibbs-Helmholtz Equation, the relationship between the equilibrium constant  $K_e^\theta(T)$  and the temperature  $T$  can be established. Details of the calculation process for  $K_e^\theta(T)$  are shown in the Supplementary Material.

The effects on the heat efficiency and the temperature difference from equilibrium of increasing the flow rate of the reactant mixture through the annular catalyst bed, with a fixed flow rate of the reactant mixture through the inner catalyst bed, at three different temperatures of the furnace chamber are shown in Fig. 9, and Figs. S5 and S6 in the Supplementary Material. The temperature difference from equilibrium gradually increased with increasing flow rate of the reactant mixture through the annular catalyst bed. This is as expected since the contact time decreases with increasing flow rate, resulting in a decrease in the conversions of methane and CO<sub>2</sub>. The heat efficiency increased gradually with increasing flow rate of reactant through the annular catalyst bed. The reason for this is that although the conversions of methane and CO<sub>2</sub> decrease, the reaction process over the catalyst bed is intensified owing to the increase in the temperature difference from equilibrium, resulting in an increase in the total conversion of the reactants. Thus the heat efficiency increases with increasing flow rate, despite the decreased conversions of methane and CO<sub>2</sub>.

The effects on the heat efficiency and the temperature difference from equilibrium of increasing the flow rate of the reactant mixture through the inner catalyst bed, with a fixed flow rate of the reactant mixture through annular catalyst bed, were also investigated at three different temperatures of the furnace chamber and the results are shown in Fig. 10, and Figs. S7 and S8 in the Supplementary Material. When the flow rate of the reactant mixture through the inner catalyst bed was increased from 191 h<sup>-1</sup> to 382 h<sup>-1</sup>, there was a negligible effect on the heat efficiency but a slight increase in the temperature difference from equilibrium. When the flow rate was further increased, the heat efficiency decreased almost in inverse proportion to the flow rate of the reactant mixture through the inner catalyst bed. A possible explanation is that the conversion of methane in the catalytic combustion remained unchanged over the range of reactant mixture flow rates employed, and as a

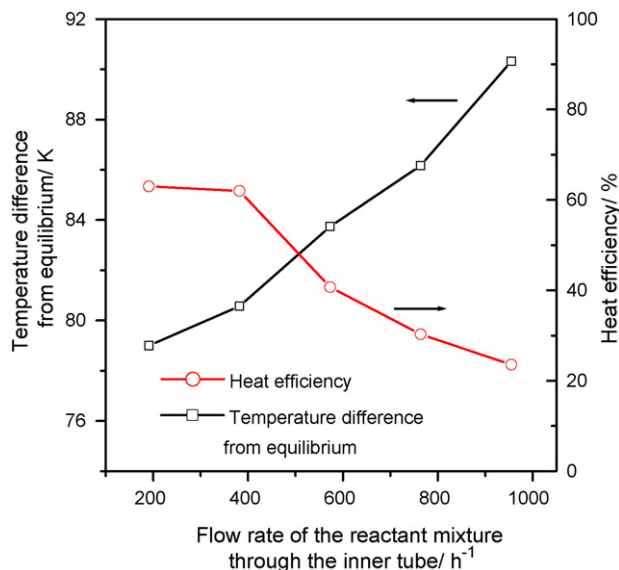


**Fig. 10.** Influence of the flow rate of the reactant mixture through the inner tube on the heat efficiency and the temperature difference from equilibrium. (The temperature of the chamber of the electric furnace was 1037 K and the flow rate of the reactant mixture through the jacket was 40 h<sup>-1</sup>.)

result the amount of heat evolved in the reaction process increased with increasing flow rate of the reactant mixture. However, the conversions of methane and CO<sub>2</sub> observed, and the corresponding amount of heat absorbed in the reforming reaction process were also essentially unchanged, given the constant flow rate of reactant mixture through annular catalyst bed. Therefore, the heat efficiency decreases rapidly. This shows that in order to achieve efficient utilization of reaction heat, the flow rate of the reactant mixture through the inner catalyst bed should be matched with that of the reactant mixture through the annular catalyst bed so as to meet the requirement of the endothermic reaction. The temperature difference from equilibrium increased gradually with increasing flow rate of reactant mixture through the inner catalyst bed for furnace chamber temperatures of 1037 K and 1139 K while a maximum in the variation of temperature difference from equilibrium with increasing flow rate was observed for a furnace chamber temperature of 1088 K. The reaction temperature has a significant effect on the temperature difference from equilibrium for both thermodynamic and kinetic reasons.

The values of the heat efficiency and the temperature difference from equilibrium at different temperatures of the furnace chamber, with constant flow rates of reactant mixture through the inner and annular catalyst beds of 382 h<sup>-1</sup> and 40 h<sup>-1</sup>, respectively, are summarized in Table 1. The heat efficiency reached 81.9% at a furnace chamber temperature of 1088 K.

**Table 1**

Influence of the temperature of the chamber of the electric furnace on the heat efficiency and the temperature difference from equilibrium<sup>a</sup>.

Temperature of the chamber of the electric furnace/K	Heat efficiency $\eta$ /%	Temperature difference from equilibrium/K
986	48.2	100
1037	62.0	81
1088	81.9	69
1139	78.4	70

<sup>a</sup> The flow rates of the reactant mixtures through the jacket and inner tube were 40 h<sup>-1</sup> and 382 h<sup>-1</sup>, respectively.

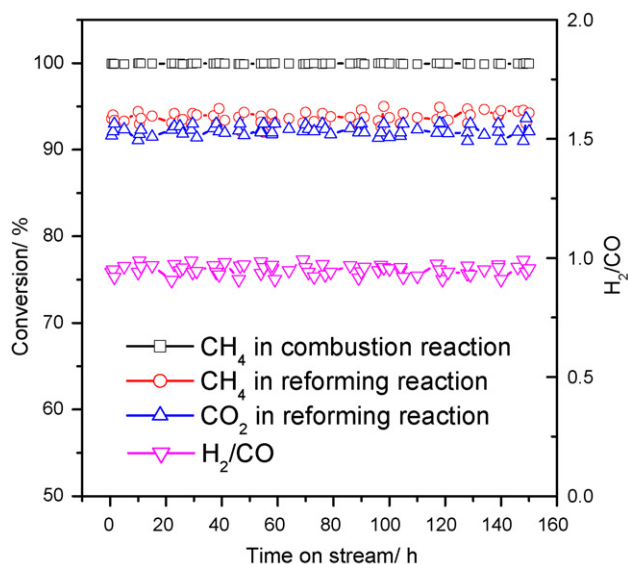


Fig. 11. Stability test of the coupling process.

### 3.3. Stability

A test of the stability of the coupled reaction system was carried out with flow rates of reactant mixture through the inner and annular catalyst beds of  $382 \text{ h}^{-1}$  and  $40 \text{ h}^{-1}$ , respectively, at a furnace chamber temperature of  $1088 \text{ K}$ . The results are shown in Fig. 11. It was found that the conversion of methane in the catalytic combustion and conversions of methane and  $\text{CO}_2$  in the reforming reaction, as well as the molar ratio of  $\text{H}_2$  to  $\text{CO}$  in the product of the reforming reaction, all remained essentially unchanged during  $150 \text{ h}$  on stream. This indicates that the inner and annular metallic monolith catalysts used in this work have good stability.

## 4. Conclusion

A preliminary study of the thermal coupling of the catalytic combustion of methane with its  $\text{CO}_2$  reforming was carried out using a tubular jacket reactor packed with metallic monolith catalysts. The main conclusions obtained are as follows:

- (1) The metallic monolith catalysts exhibit good catalytic activities. In the jacket reactor packed with these catalysts, the heat absorbed by the reforming of methane with  $\text{CO}_2$  is indeed partly provided by the heat evolved in the catalytic combustion of methane over a wide range of experimental conditions, and so the direct heat coupling of the two reactions has been realized on the laboratory scale.
- (2) The flow rates of reactant mixtures through the inner and annular catalyst beds should be matched in order to retain high conversions of methane and  $\text{CO}_2$  in the methane reforming reaction and to produce large amounts of hydrogen. For example, as a result of limits by imposed thermodynamics and kinetics, for a furnace chamber temperature of  $1088 \text{ K}$  and a flow rate of reactant mixture through the inner catalyst bed of  $764 \text{ h}^{-1}$ , conversions of methane and  $\text{CO}_2$  higher than  $90\%$  and molar ratios of  $\text{H}_2$  to  $\text{CO}$  higher than  $0.8$  could only be reached when flow rate of reactant mixture through the annular catalyst bed was below  $50 \text{ h}^{-1}$ .
- (3) For a furnace chamber temperature of  $1088 \text{ K}$  and flow rates of reactant mixtures through the inner and annular catalyst beds

of  $382 \text{ h}^{-1}$  and  $40 \text{ h}^{-1}$  respectively, the conversions of methane and  $\text{CO}_2$  in the reforming reaction reached  $93.6\%$  and  $91.7\%$ , respectively. The molar ratio of  $\text{H}_2$  to  $\text{CO}$  in the product gas under the same conditions was about  $0.85$ .

- (4) The metallic monolith catalysts exhibited good stability, and did not deactivate during  $150 \text{ h}$  on stream.

All of these results should be considered to be preliminary in view of the fact that the heat capacity of the laboratory reactor is very much smaller than that of the furnace, the radiative heat transfer from the furnace body (which will have a temperature slightly higher than those of the annular catalyst bed and the furnace chamber) to the reactor cannot be ignored or measured accurately, and especially as the temperatures at the inlet and outlet of both the exothermic and endothermic reaction compartments as well as the temperature profiles were not measured. Further detailed investigation of such systems is needed.

## Acknowledgements

Financial support from the National Natural Science Foundation of China (Project No. 20136010) and the National Basic Research Program of China (Project No. 2005CB221405) are gratefully acknowledged.

## Appendix A. Supplementary data

Supplementary data associated with this article can be found, in the online version, at doi:10.1016/j.cej.2009.03.029.

## References

- [1] A. Stankiewicz, J.A. Moulijn, *Ind. Eng. Chem. Res.* 41 (2002) 1920.
- [2] J. Frauhammer, G. Eigenberger, L.V. Hippel, D. Arntz, *Chem. Eng. Sci.* 54 (1999) 3661.
- [3] G. Kolios, J. Frauhammer, G. Eigenberger, *Chem. Eng. Sci.* 55 (2000) 5945.
- [4] M. van Sint Annaland, R.C. Nijssen, *Chem. Eng. Sci.* 57 (2002) 4967.
- [5] M. van Sint Annaland, H.A.R. Scholts, J.A.M. Kuipers, W.P.M. van Swaaij, *Chem. Eng. Sci.* 57 (2002) 833.
- [6] M. van Sint Annaland, H.A.R. Scholts, J.A.M. Kuipers, W.P.M. van Swaaij, *Chem. Eng. Sci.* 57 (2002) 855.
- [7] V.R. Choudhary, S.A.R. Mulla, V.H. Rane, *Appl. Energy* 66 (2000) 51.
- [8] V.R. Choudhary, V.H. Rane, A.M. Rajput, *Ind. Eng. Chem. Res.* 39 (2000) 904.
- [9] L. Ma, D.L. Trimm, *Appl. Catal. A: Gen.* 138 (1996) 265.
- [10] V.H. Rane, A.M. Rajput, A.J. Karkamkar, V.R. Choudhary, *Appl. Energy* 77 (2004) 375.
- [11] L. Baitao, M. Kenji, N. Mohammad, K. Kimio, T. Keiichi, *Appl. Catal. A: Gen.* 275 (2004) 157.
- [12] B. Glockler, G. Kolios, G. Eigenberger, *Chem. Eng. Sci.* 58 (2003) 593.
- [13] M.S. Kulkarni, M.P. Dudukovic, *AIChE J.* 42 (1996) 2897.
- [14] M.S. Kulkarni, M.P. Dudukovic, *Chem. Eng. Sci.* 52 (1997) 1777.
- [15] A.Y. Tonkovich, S. Perry, Y. Wang, D. Qiu, T. LaPlante, W.A. Rogers, *Chem. Eng. Sci.* 59 (2004) 4819.
- [16] T. Ioannides, X.E. Verykios, *Catal. Today* 46 (1998) 71.
- [17] Z.R. Ismagilov, V.V. Pushkarev, O.Y. Podyacheva, N.A. Koryabkina, H. Veringa, *Chem. Eng. J.* 82 (2001) 355.
- [18] M. Zafir, A. Gavriilidis, *Chem. Eng. Sci.* 56 (2001) 2671.
- [19] M. Zafir, A. Gavriilidis, *Chem. Eng. Sci.* 57 (2002) 1653.
- [20] M. Zafir, A. Gavriilidis, *Chem. Eng. J.* 86 (2002) 277.
- [21] M. Zafir, A. Gavriilidis, *Chem. Eng. Sci.* 58 (2003) 3947.
- [22] F.A. Robbins, H. Zhu, G.S. Jackson, *Catal. Today* 83 (2003) 141.
- [23] T. Giroux, S. Hwang, Y. Liu, W. Ruettinger, L. Shore, *Appl. Catal. B: Environ.* 56 (2005) 95.
- [24] B. Kucharczyk, W. Tylus, L. Kepinski, *Appl. Catal. B: Environ.* 49 (2004) 27.
- [25] F. Yin, S. Ji, N. Chen, M. Zhang, L. Zhao, C. Li, H. Liu, *Catal. Today* 105 (2005) 372.
- [26] F. Yin, S. Ji, B. Chen, L. Zhao, H. Liu, C. Li, *Appl. Catal. B: Environ.* 66 (2006) 264.
- [27] F. Yin, S. Ji, B. Chen, Z. Zhou, H. Liu, C. Li, *Appl. Catal. A: Gen.* 310 (2006) 164.
- [28] H. Mei, C. Li, H. Liu, *Catal. Today* 105 (2005) 689.
- [29] H. Mei, C. Li, S. Ji, H. Liu, *Chem. Eng. Sci.* 62 (2007) 4294.
- [30] M. Zhang, S. Ji, L. Hu, F. Yin, C. Li, H. Liu, *Chin. J. Catal.* 27 (2006) 777.